Volume 10, Issue 2, 2020, 5091 - 5095 ISSN 2069-5837
Biointerface Research in Applied Chemistry
www.BiointerfaceResearch.com
https://doi.org/10.33263/BRIAC0102.091095
Original Research Article Open Access Journal
Received: 06.01.2020 / Revised: 24.01.2020 / Accepted: 25.01.2020 / Published on-line: 28.01.2020

Mapping molecular electrostatic potential for heme interacting with nano metal oxides

Ahmed M. Bayoumy[1], Hanan Elhaes [2], Osama Osman [3], Tarek Hussein[4], Medhat A. Ibrahim [3,*]
[1]Physics Department, Biophysics Branch, Faculty of Science, Ain Shams University, 11566, Cairo, Egypt
[2]Physics Department, Faculty of Women for Arts, Science and Education, Ain Shams University, 11757 Cairo, Egypt
[3]Spectroscopy Department, National Research Centre, 33 El-Bohouth Str. 12622 Dokki, Giza, Egypt
[4]Physics Department, faculty of Science, Cairo University, 12613 Giza Egypt
*corresponding author e-mail address: ***medahmed6@yahoo.com*** | Scopus ID 8641587100

ABSTRACT
Interacting various living components with several materials in the gaseous nanoscale form has been of great concern as they are utilized in different life aspects. This work is conducted to assess the impact of interacting heme molecule, the main constituent of blood hemoglobin, with various common and non-common divalent molecules such as O_2, CO_2, CO, MgO, CoO, NiO, CuO and ZnO. Calculations are calculated at DFT high theoretical level using B3LYP/SDD method. In addition, molecular electrostatic potential (MESP) maps are constructed. Results demonstrate that interacting heme with proposed various structures lowers their energies reflecting more stability. However, the addition of non-familiar species to heme makes it more stable that may affect its transportation function for O_2 and CO_2 in the presence of these toxic materials in the gaseous state. The calculated TDM of the various proposed structures indicates that they are all more reactive than heme, since TDM of all of them are larger than that of pure heme. MESP maps show that extreme negative electrostatic regions are concentrated around C=O group of terminal carboxyl groups suggesting electrophilic interactions to take place there while positive regions are found around Fe central atom and on the circumference of all the proposed structures that are occupied by H atoms increasing the probability of nucleophilic reactions in these regions. Therefore, presence of such hazardous materials in the gaseous nanoscale may impact negatively the transportation function of heme.
Keywords: *Heme; DFT; Molecular Electrostatic Potential (MESP); B3LYP.*

1. INTRODUCTION
Molecular modelling with different methods and levels is widely used to investigate different molecular properties including structure, dynamics, surface properties, and thermodynamics of huge number of systems [1-4]. Such class of computational methods is now routinely used to model or mimic the behavior of molecules to investigate their physical, chemical and biological features in different fields of science and applications [5-11]. Among the amazing properties investigated with molecular modeling, the molecular electrostatic potential (MESP). Mapping MESP for the given structure is an important step to describe the active sites of such structure [12]. It is a useful concept since it may provide information about the interaction active sites of various chemical structures [13]. Also, it is useful in determining the nature of chemical addition through which a molecule is most probable to undergo; either electrophilic or nucleophilic addition. The molecular surface has several definitions. Some scientists consider MESP as the external area of a molecule formed by a set of intersecting spheres whose centers are aligned with the nucleus of each atom [14–19]; such spheres result from the van der Waals radii of the considered atoms [20]. Another definition for MESP, introduced by Bader et al. [21, 22], states that it is the outer contour of the electronic density ρ(r) of a molecule. Many researchers prefer the later point of view than the first one since it gives more detailed characteristics of the interested structure such as σ-holes presence, lone pair electrons and many more. Several researchers ensured that these contours comprise about 95–98% of the electronic density of a molecule [20, 21]. The electrostatic potential V(r) of a molecule always confirms a significant role in guiding its reactive behavior. For biological as well as organic molecules, MESP gives significant descriptions for such molecules and considered excellent descriptors for their possible interactions [23-31].

Depending on the previous considerations, molecular modeling concepts are conducted, to continue our previous work in such research area [32, 33], for mapping the molecular electrostatic potential (MESP) of heme molecule interacting with various structures involving O_2, CO_2, CO, MgO, CoO, NiO, CuO and ZnO as samples for familiar and non- familiar species. Model molecule of heme molecule (H) interacting with each of the selected molecules using DFT high theoretical level at B3LYP method and SDD as a basis set is proposed as both adsorb and complex states.

2. MATERIALS AND METHODS
Calculation Details.
The studied structures are subjected to Density Functional Theory (DFT) at B3LYP method and Stuttgart-Dresden (SDD) effective core pseudopotential (ECP) as a basis set [34-36] via GAUSSIAN 09 Software that is implemented at Spectroscopy Department, National Research Centre, NRC [37]. Model molecules of pure heme molecule (H) and heme interacting with several common and non-common structures via both adsorption and complex states are built up. Heme molecule interacts with the added structures through its Fe atom. The chosen species are O_2, CO_2 and CO as familiar structures and MgO, CoO, NiO, CuO and ZnO as non-common ones. Some physical parameters such as total energy (E), total dipole moment (TDM) and HOMO/LUMO band gap energy (ΔE) are considered. Then, molecular electrostatic

potential (MESP) maps are constructed in order to determine the active sites of the constructed structures at the same level.

3. RESULTS

Building Model Molecules.

The model molecule of heme (H) based on our previous research work in [32, 33] . Heme structure consists of porphyrin which is a ring-like organic structure and owns a central iron (Fe) atom which represents its active site where it can bind to either oxygen (O_2) or carbon dioxide (CO_2) gases in reverse physical processes to satisfy its function of transportation. **Figure 1** shows the molecular electrostatic potential (MESP) maps of heme structure as well as its suggested interactions with O_2, CO_2, CO, MgO, CoO, NiO, CuO and ZnO through its Fe active site.

Geometry Optimization.

All calculations are carried out in order to investigate the impact of binding various species with heme on its physical and electronic properties. Calculations are conducted at high theoretical DFT level using B3LYP/SDD method. **Table 1** lists three physical parameters such as total energy (E), total dipole moment (TDM) and HOMO/LUMO band gap energy (ΔE).

It is well-known that the total energy of a structure reflects its stability whereas the structure's energy decreases, its stability increases with respect to others. The energy of heme molecule is about -53.2862 keV. The addition of various entities to its structure makes it more stable, since all the presented energies, in **table 1**, of all the considered structures are lower than that of the heme. It is worth to notice that the resultant energy of each of the added structures to heme as adsorb state nearly equals the corresponding one in the complex one. Energies of heme bonded to O_2, CO_2 and CO are the highest among the proposed structures with respect to others. However, the addition of other species to heme makes it more stable that may affect its O_2 and CO_2 transportation function in the presence of these toxic materials in the gaseous state. Energies of heme bonded to MgO, CuO and ZnO are the lowest among the proposed structures with respect to others. Total dipole moment (TDM) as well as HOMO/LUMO band gap energy (ΔE) are considered powerful physical indicators for the reactivity of a certain structure. The calculated TDM for heme is 4.3580 Debye. The calculated TDM of the various proposed structures indicates that they are all more reactive than heme, since their TDMs of all of them are larger than that of pure heme. In addition, results of TDM of heme bonded to various molecules in the complex state is higher than those in the adsorb state except for heme bonded to CO that has the least TDM and hence reactivity. TDM of heme bonded to O_2, CO_2 and CO are smaller than other non-familiar structures that may help heme in its transportation function. High TDM of heme bonded to MgO, CuO, NiO, CoO and ZnO indicates highly reactive structures, however, it may disturb transportation function of heme. TDM of heme bonded to MgO and CuO in the adsorbed state is the highest, however, TDM of heme bonded to MgO, CuO and ZnO are the largest in the complex state. HOMO/LUMO band gap energy of heme is 0.076eV that lowers when interacting with the proposed structures via either adsorb or complex states except for heme complexed with CO. This reflects higher electrical conductivity for these structures. Heme bonded to MgO and CuO has the least band gaps in the adsorb states while heme bonded to CoO has the smallest one in the complex state.

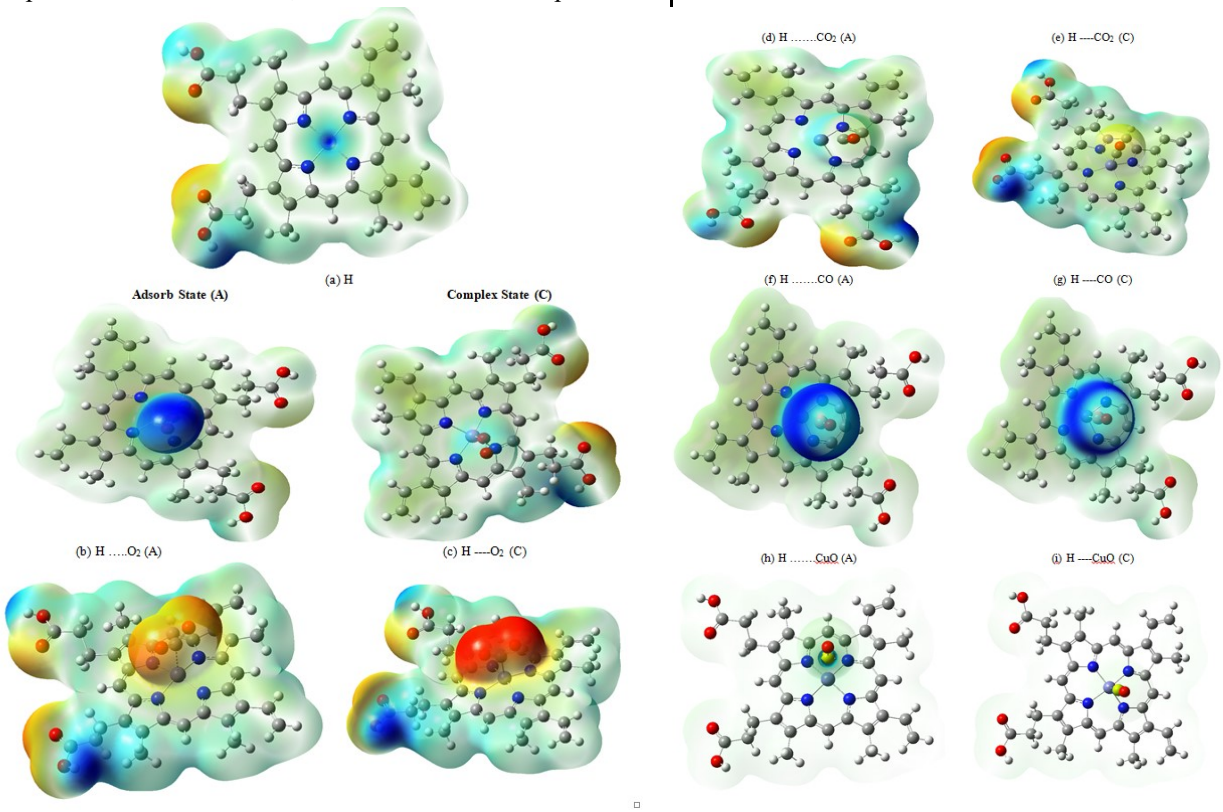

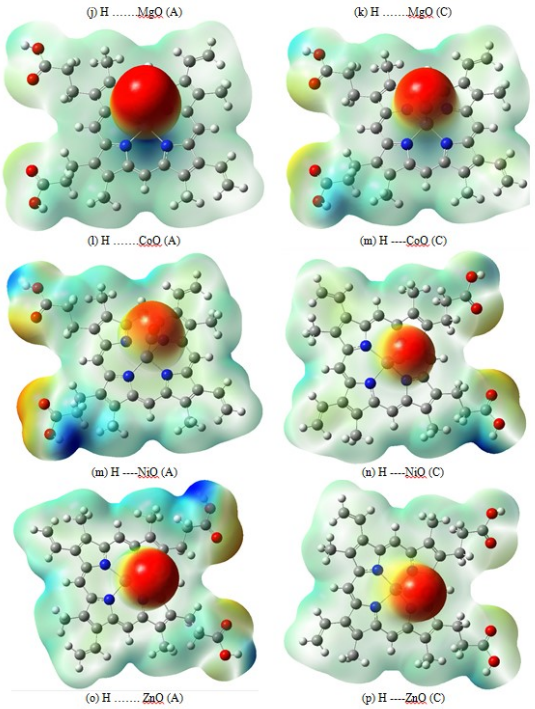

Figure 1. Calculated molecular electrostatic potential (MESP) maps of (a) heme molecule (H), and its interaction with O_2, CO_2, CO, MgO, CoO, NiO, CuO and ZnO as adsorb state (A) on the left hand side and complex state on the right hand side (C) on DFT using B3LYP/SDD method.

Table 1. DFT calculated energy (E) as eV, total dipole moment (TDM) as Debye and band gap energy as eV for heme molecule and its interaction structures with O_2, CO_2, CO, MgO, CoO, NiO, CuO and ZnO as adsorb and complex states using B3LYP/SDD method.

Structure	E (keV)	TDM (Debye)	ΔE (eV)
H	-53.2862	4.3580	0.0670
Interaction as adsorption			
H-O_2	-57.3753	6.6084	0.0231
H-CO_2	-58.4152	7.2837	0.053
H-CO	-56.3689	5.7604	0.0578
H-MgO	-60.7764	9.9141	0.0066
H-CoO	-59.3020	8.1830	0.0552
H-NiO	-59.9826	7.8839	0.0461
H-CuO	-60.7031	9.5691	0.0086
H-ZnO	-61.5127	8.9374	0.0428
Interaction as complex			
H-O_2	-57.3768	6.7087	0.0456
H-CO_2	-58.4142	7.9925	0.0309
H-CO	-56.3711	5.6859	0.0906
H-MgO	-60.7765	10.3648	0.0318
H-CoO	-59.3020	8.6763	0.0002
H-NiO	-59.9823	8.5375	0.0343
H-CuO	-60.7032	10.1990	0.0126
H-ZnO	-61.5119	10.9866	0.0368

Molecular electrostatic potential (MESP) maps.

Molecular electrostatic potential (MESP) maps are constructed for the suggested structures at DFT level at B3LYP/SDD method in both adsorb and complex states. MESP maps offer simple and quite good method for illustrating charge distribution through a chemical structure and hence its active sites. Figure 1 shows the molecular electrostatic potential (MESP) maps for heme structure as well as its suggested interactions with O_2, CO_2, CO, MgO, CoO, NiO, CuO and ZnO through its Fe active site. The resultant MESP maps are characterized by consisting of various colors ranging from red to dark blue indicating the extreme negative and positive sites, respectively in the interested structure. The complete map configuration contains colors in the order of red, orange, yellow, green, light blue and dark blue from the most negative to most positive. Red color corresponds to the extreme negative potentials while dark blue one for extreme positive ones. Yellow color is a less negative potential region with respect to the red one. Similarly, light blue regions are of less positive potentials than the dark blue ones. Green color indicates regions of nearly neutral potentials relative to both red and dark blue ones. The distribution of potentials as well as colors can be related in some way by the relation between electronegativity of the bonded atoms. Highly electronegative atoms will be colored by red when bonded with less electronegative ones. Having atoms of close electronegative values makes the color distribution to be much narrower. Therefore, MESP maps can be utilized as physical property in determining whether the active sites of the interesting chemical structures can undergo either nucleophilic or electrophilic interactions. In this study, MESPs are presented as mapped surfaces for all the proposed model molecules. The

constructed MESP maps of heme and its various interactions either in adsorb or complex states have general features. Extreme negative electrostatic regions are concentrated around C=O group of terminal carboxyl groups of heme structure suggesting electrophilic interactions to take place there. While positive regions are found on the circumference of all the proposed structures that are occupied by H atoms increasing the probability of nucleophilic reactions in these regions. Their colors range from green to dark blue in some structures. For pristine heme molecule, there is clear color distribution where its central Fe atom appears in blue referring to positive region. Other regions appear in different colors range from yellow to light blue indicating neutral to quite positive areas. The addition of various molecules through either adsorb or complex states modifies the MESP maps of most of the proposed models. Oxygen addition to heme in the adsorbed state creates extreme positive region in the interaction site and light blue in other regions even around C=O ones. While its addition in the complex state has no significant impact on the electronegative regions in the structure. Similarly, addition of CO, CuO and MgO create either light blue or dark blue areas around Fe interaction site in both adsorb and complex states. However, CO addition has little impact on the electrostatic negative regions, the addition of both CuO and MgO affect greatly the electronegativity of C=O group. While addition of CO_2, CoO, NiO and ZnO species to heme creates a highly electronegative region around Fe active site. This can be attributed to the difference in the electronegativity between oxygen atom and C, Co, Ni and Zn atoms. These additions have little effect in the electrostatic charge distribution across heme molecule.

4. CONCLUSIONS

The current work investigated the physical properties as well as constructed molecular electrostatic (MESP) maps of heme structure and heme bonded with common and non-common divalent molecules using DFT high level at B3LYP/SDD method. Structures such as O_2, CO_2, CO, MgO, CoO, NiO, CuO and ZnO are added to heme. Heme interacted with these structures through its Fe atom as both adsorb and complex states. Results demonstrate that interacting heme with proposed various structures lowers their energies reflecting more stability. However, the addition of non-familiar species to heme makes it more stable that may affect its O_2 and CO_2 transportation function in the presence of these toxic materials in the gaseous state. The calculated TDM of the various proposed structures indicates that they are all more reactive than heme, since TDM of all of them are larger than that of pure heme. High TDM of heme bonded to MgO, CuO, NiO, CoO and ZnO indicates highly reactive structures, however, it may disturb transportation function of heme. MESP maps show that extreme negative electrostatic regions are concentrated around C=O group of terminal carboxyl groups suggesting electrophilic interactions to take place there while positive regions are found around Fe central atom and on the circumference of all the proposed structures that are occupied by H atoms increasing the probability of nucleophilic reactions in these regions. While addition of CO_2, CoO, NiO and ZnO species to heme creates a highly electronegative region around Fe active site. This is attributed as mentioned earlier to the difference in the electronegativity between oxygen atom and C, Co, Ni and Zn atoms. Therefore, the presence of such hazardous materials in the gaseous nanoscale may impact negatively the transportation function of heme.

5. REFERENCES

1. Ahlawat, S.; Singh, D.; Virdi, J.S.; Sharma, K.K. Molecular modeling and MD-simulation studies: Fast and reliable tool to study the role of low-redox bacterial laccases in the decolorization of various commercial dyes. *Environ. Pollut.* **2019**, *253*, 1056-1065, https://doi.org/10.1016/j.envpol.2019.07.083.
2. Kushwaha, A.; Gupta, N.; Srivastava, J.; Singh, A.K.; Singh, M. Development of highly sensitive and selective sensor for ethionamide guided by molecular modelling via electropolymerized molecularly imprinted films. *Microchem. J.* **2020**, *152*, 104355, https://doi.org/10.1016/j.microc.2019.104355.
3. Spaggiari, G.; Pizio, A.D.; Cozzini, P. Sweet, umami and bitter taste receptors: State of the art of in silico molecular modeling approaches. *Trends in Food Sci.Technol.* **2020**, *96*, 21-29, https://doi.org/10.1016/j.tifs.2019.12.002,
4. Ahmad, S.; Bhagwati, S.; Kumar, S.; Banerjee, D.; Siddiqi, M.I. Molecular modeling assisted identification and biological evaluation of potent cathepsin S inhibitors. *J. Mol. Graph. Model.* **2020**, *96,* 107512, https://doi.org/10.1016/j.jmgm.2019.107512.
5. Ibrahim, M. Molecular Modelling and FTIR Study for K, Na, Ca and Mg Coordination with Organic Acid. *J. Comput. Theor. Nanosci.* **2009**, *6*, 682–685, https://doi.org/10.1166/jctn.2009.1094.
6. Fahim, A.M.; Shalaby, M.A.; Ibrahim, M. Microwave-assisted synthesis of novel 5-aminouracil-based compound with DFT calculations. *J. Mol. Struct*. **2019**, *1194*, 211-226, https://doi.org/10.1016/j.molstruc.2019.04.078.
7. Grenni, P.; Caracciolo, A.B.; Mariani, L.; Cardoni, M.; Riccucci, C.; Elhaes, H.; Ibrahim, M.A. Effectiveness of a new green technology for metal removal from contaminated water. *Microchem. J.* **2019**, *147*, 1010-1020, https://doi.org/10.1016/j.microc.2019.04.026.
8. Alaaeldin, G.M.F.; Atta, D.; Abouelsayed, A.; Ibrahim, M.A.; Hanna, A.G. Configuration and Molecular Structure of 5-Chloro-N-(4-sulfamoylbenzyl) Salicylamide Derivatives. *Spectrochim. Acta A*. **2019**, *214*, 476–486, https://doi.org/10.1016/j.saa.2019.02.070.
9. Abdelsalam, H.; Teleb, N.H.; Yahia, I.S.; Zahran, H.Y.; Elhaes, H.; Ibrahim, M.A. First principles study of the adsorption of hydrated heavy metals on graphene quantum dots. *J. Phys. Chem. Solids* **2019**, *130*, 32-40, https://doi.org/10.1016/j.jpcs.2019.02.014.
10. Youness, R.A.; Taha, M.A.; Elhaes, H.; Ibrahim, M. Molecular Modeling, FTIR Spectral Characterization and Mechanical Properties of Carbonated-Hydroxyapatite Prepared by Mechanochemical Synthesis. *Mater. Chem. Phys.* **2017**, *190,* 209-218, https://doi.org/10.1016/j.matchemphys.2017.01.004.
11. Bayoumy, A.M.; Refaat, A.; Yahia, I.S., Zahran, H.Y.; Elhaes H.; Ibrahim, M.A.; Shkir, M. Functionalization of Graphene Quantum Dots (GQDs) with Chitosan Biopolymer for Biophysical Applications. *Opt.Quant. Electron.* **2020,** *52,* 16, https://doi.org/10.1007/s11082-019-2134-z.

12. Ezzat, H.; Badry, R.; Yahia, I.S.; Zahran, H.Y.; Ibrahim, A.; Elhaes, H.; Ibrahim, M.A. Mapping the molecular electrostatic potential of fullerene. *Egypt. J. Chem*. **2019**, *6*, 1391-1402, https://dx.doi.org/10.21608/ejchem.2019.5353.1472.
13. Bulat, F.A.; Toro-Labbe, A.; Brinck, T.; Murray, J.S.; Politze, P. Quantitative analysis of molecular surfaces: areas, volumes, electrostatic potentials and average local ionization energies. *J. Mol. Model.* **2010**, *16*, 1679-1691, https://doi.org/10.1007/s00894-010-0692-x.
14. Lee, B.; Richards, F.M. The interpretation of protein structures: estimation of static accessibility. *J. Mol. Biol.* **1971**, *55*, 379-IN4, https://doi.org/10.1016/0022-2836(71)90324-X.
15. Weiner, P.K.; Langridge, R.; Blaney, J.M.; Kollma, P.A. Electrostatic potential molecular surfaces. *Proc. Nat. Acad. Sci.* **1982**, *79*, 3754-3758, https://dx.doi.org/10.1073%2Fpnas.79.12.3754.
16. Connolly, M.L. Solvent-accessible surfaces of proteins and nucleic acids. *Sci.* **1983**, *221*, 709-713, https://doi.org/10.1126/science.6879170.
17. Francl, M.M.; Hout, Jr.R.F.; Hehre, W.J. Representation of electron densities. 1. Sphere fits to total electron density surfaces. *J. Am. Chem. Soc.* **1984**. *106*, 563-570, https://doi.org/10.1021/ja00315a018.
18. Arteca, G.A.; Jammal, V.B.; Mezey, P.G.; Yadav, J.S.; Hermsmeier, M.A.; Gund, T.M. Shape group studies of molecular similarity: Relative shapes of Van der Waals and electrostatic potential surfaces of nicotinic agonists. *J. Mol. Graph.* **1988**, *6,* 45-53, https://doi.org/10.1016/0263-7855(88)80061-4.
19. Dunitz, J.D.; Filippini, G.; Gavezzotti, A. A statistical study of density and packing variations among crystalline isomers. *Tetrahedron* **2000**, *56*, 6595-6601, https://doi.org/10.1016/S0040-4020(00)00460-9.
20. Bondi, A. van der Waals volumes and radii. *J. Phys. Chem.* **1964**. *68,* 441-451, https://doi.org/10.1021/j100785a001.
21. Bader, R.; Henneker, W.H.; Cade, P.E. Molecular charge distributions and chemical binding. *J. Chem. Phys.* **1967**, *46*, 3341-3363, https://doi.org/10.1063/1.1841222.
22. Bader, R.F.; Caroll, M.T.; Cheeseman, J.R.; Chang, C. Properties of atoms in molecules: atomic volumes. *J. Am. Chem. Soc.* **1987**,*109*, 7968-7979, https://doi.org/10.1021/ja00260a006.
23. Homouz, D.; Joyce-Tan, K.H.; Shamsir, M.S.; Moustafa, I.M.; Idriss, H.T. Molecular dynamics simulations suggest changes in electrostatic interactions as a potential mechanism through which serine phosphorylation inhibits DNA polymerase β activity. *J. Mol. Graph. Model.* **2018,** *84*, 236-241, https://doi.org/10.1016/j.jmgm.2018.08.007.
24. Wu, S.; Zhang, W.; Qi, L.; Ren, Y.; Ma, H. Investigation on 4-amino-5-substituent-1,2,4-triazole-3-thione Schiff bases an antifungal drug by characterization (spectroscopic, XRD), biological activities, molecular docking studies and electrostatic potential (ESP*). J. Mol. Struct.* **2019**, *1197*, 171-182, https://doi.org/10.1016/j.molstruc.2019.07.013.
25. Pramanik, S.; Dey, T.; Mukherjee, A.K. Five benzoic acid derivatives: Crystallographic study using X-ray powder diffraction, electronic structure and molecular electrostatic potential calculation. *J. Mol. Struct.* **2019**, *1175*, 185-194, https://doi.org/10.1016/j.molstruc.2018.07.090.
26. Cruz, J.C.; Hernández-Esparza, R.; Vázquez-Mayagoitia, Á.; Vargas, R.; Garza, J. Implementation of the Molecular Electrostatic Potential over Graphics Processing Units. J. Chem. Inf. Model. **2019**, 59, 7, 3120-3127**.** https://doi.org/10.1021/acs.jcim.8b00951
27. Kumar, P.; Gruza, B.; Bojarowski, S.A.; Dominiak, P.M. Extension of the transferable aspherical pseudoatom data bank for the comparison of molecular electrostatic potentials in structure–activity studies. Acta Cryst. **2019**, A**75**, 398-408. https://doi.org/10.1107/S2053273319000482
28. Iruthayaraj, A.; Chinnasamy, K.; Jha, K.K.; Munshi, P.; Pavan, M.S.; Kumaradhas, P. Topology of electron density and electrostatic potential of HIV reverse transcriptase inhibitor zidovudine from high resolution X-ray diffraction and charge density analysis. J. Mol. Struct. 2019, 1180, 683-697. https://doi.org/10.1016/j.molstruc.2018.11.098
29. Mehmood, A.; Jones, S.I.; Tao, P.; Janesk, B.G. An Orbital-Overlap Complement to Ligand and Binding Site Electrostatic Potential Maps. J. Chem. Inf. Model. **2018**, 58, 9, 1836-1846. https://doi.org/10.1021/acs.jcim.8b00370
30. Yao, H.; Qian, D.; Zhang, H.; Qin, Y.; Xu, B.; Cui, Y.; Yu, R.; Gao, F.; Hou, J. Critical Role of Molecular Electrostatic Potential on Charge Generation in Organic Solar Cells. Chin. J. Chem. **2018**, 36 (6), 491-494. https://doi.org/10.1002/cjoc.201800015
31. Raghi, K.R.; Sherin, D.R.; Saumya, M.J.; Arun, P.S.; Sobha, V.N.; Manojkumar, T.K. Computational study of molecular electrostatic potential, docking and dynamics simulations of gallic acid derivatives as ABL inhibitors. Comput. Biol. Chem. **2018** 74, 239-246. https://doi.org/10.1016/j.compbiolchem.2018.04.001
32. Elhaes, H.; Osman, O.; Ibrahim, M. Interaction of Nano Structure Material with Heme Molecule: Modelling Approach. *J Comput Theor Nanosci.* **2012**, *9*, 901–905, https://doi.org/10.1166/jctn.2012.2114.
33. Bayoumy, A.M.; Elhaes, H.; Osman, O.; Kholmurodov, K.T.; Hussein, T.; Ibrahim, M.A. Effect of Nano Metal Oxides on Heme Molecule: Molecular and Bimolecular Approaches. *Biointerface Res. Appl. Chem.* **2020**, *10*, 1, 4837-4845.
34. Becke, A.D. Density-functional thermochemistry. III. The role of exact exchange. *J. Chem. Phys.* **1993**, *98*, 5648–5652, https://doi.org/10.1063/1.464913.
35. Lee, C.; Yang, W.; Parr, R.G. Development of the Colic-Salvetti correlation-energy formula into a functional of the electron density. *Phys. Rev. B* **1988**, *37,* 785, https://doi.org/10.1103/PhysRevB.37.785.
36. Vosko, S.H.; Wilk, L.; Nusair, M. Accurate spin-dependent electron liquid correlation energies for local spin density calculations: a critical analysis. *J. Phys.* **1980**, *58*, 1200–1211, https://doi.org/10.1139/p80-159.
37. Frisch, M.J.; et al. Gaussian, Inc., Wallingford CT, **2010**.

6. ACKNOWLEDGEMENTS

This work is carried out in the frame of the ASRT-JINR bilateral project “Molecular Modeling Analyses of the Effect of Nano Metal Oxides on Biological Molecules”.